0022-538X/78/0025-0339$02.00/0
JOURNAL OF VIROLOGY, Jan. 1978, p. 339-348

Vol. 25, No. 1
Printed in U.S.A.

Comparison of Two Viable Variants of Simian Virus 40

ALAN C. KAY, G. R. KOTESWARA RAO†, AND MAXINE F. SINGER*
Laboratory of Biochemistry, National Cancer Institute, Bethesda, Maryland 20014

Received for publication 19 July 1977

The DNAs of two viable strains of simian virus 40, 776 and 777, have been compared by using restriction endonucleases. Differences between the two strains were detected at five separate points on the simian virus 40 genome. One of these differences, in the region of DNA coding for the major viral coat protein, was confirmed by tryptic peptide analysis of coat proteins from the two strains. Some physiological differences between the two strains were examined and can, in general, be explained by differences observed between the DNAs of the two strains. In addition, defective variants derived from strain 777 interfere more efficiently with the replication of strain 777 than with the replication of strain 776.

The existence of viable variant strains of simian virus 40 (SV40) that differ in plaque size, oncogenicity, and temperature sensitivity (34), as well as in host range (22) and in immunological properties (23), has been known for some time. The variants have been designated as large-, small-, or minute-plaque strains. Some strains have more precise designations (e.g., 776, 777, Rh 911, etc.). Differences in the size of some of the fragments produced from the DNA of variants by combined action of the restriction endonucleases *Hin*dII and *Hin*dIII (endo R · *Hin*dII/R · *Hin*dIII [32]) have been observed (19, 20), and electrophoretic differences have been found between the major capsid proteins of large and small-plaque strains (1).

Maps of the digestion products of SV40 DNA by various restriction enzymes are now available, including those of endoR · *Hin*dII, R · *Hin*dIII (5, 37), R · *Eco*RII (33), R · *Hae* III (33, 38), and R · *Alu* I (12, 39). Also, genetic analyses and transcription studies have indicated the approximate regions coding for the four known viral-coded proteins: T-antigen, VP1, VP2, and VP3 (3, 13, 35), and these studies have been confirmed and extended by complementation of temperature-sensitive mutants with wild-type restriction fragments (15) by linked transcription-translation of viral proteins from restriction fragments (29) and by nucleotide sequence determination (36). It is, therefore, now possible to correlate directly differences between variant DNAs as seen in restriction endonuclease studies with alterations in viral-coded proteins and attempt to explain physiological variations between virus strains.

† Present address: Department of Biochemistry, Institute of Medical Sciences, Banaras Hindu University, Varanasi, 221005 India.

We report here more detailed analyses of a large-plaque strain (777) and a small-plaque strain (776), using endonucleases R · *Hin*dII, R · *Hin*dIII, R · *Hae* III, and R · *Alu* I. The differences between the two strains were located on the SV40 map. One particular difference in the region coding for viral coat protein was confirmed by demonstrating differences between the tryptic peptide patterns of the two isolated viral proteins.

MATERIALS AND METHODS

Cells and virus stocks. All experiments were carried out with the BSC-1 line of monkey kidney cells. Cells were cultured as described previously (17). Stocks of plaque-purified SV40, strains 776 and 777, were kindly provided by Daniel Nathans and Ernest Winocour, respectively. The plaque from which the 777 stock was derived was named CVB (16). New stocks were prepared in this laboratory by infecting confluent monolayers of BSC-1 cells at multiplicities of infection (MOI) of less than 10^{-3} PFU/cell. When the cytopathic effect was complete, the lysates were collected and treated as previously described (16). Virus was titrated by plaque assay on BSC-1 monolayers (16).

Defective virus stocks were all derivatives of the passage series designated CVB, series one in previous papers, and the series was originally initiated with a stock of CVB (777), (16, 25, 28).

Labeling of cultures and preparation of labeled DNA for rate studies. At various times after infection (times indicated with each experiment), the medium was removed from plates and replaced with identical fresh medium (modified Eagle no. 2 with 2% bovine fetal serum) containing 10 μCi of [*methyl*-^{3}H]thymidine (about 20 Ci/mmol, New England Nuclear Corp., Boston, Mass.) per ml. After further incubation at 37°C for the times indicated in each experiment, the radioactive medium was removed, the cells were washed twice with ice-cold phosphate-

buffered saline, and viral DNA was isolated by the procedure of Hirt (10). Samples of the Hirt supernatant fluids were made 1 M in NaOH, incubated at 100°C for 20 min and neutralized with HCl, and then DNA was precipitated by addition of an equal volume of 20% trichloroacetic acid. More than 95% of the DNA in the supernatant fraction obtained by the Hirt procedure from SV40-infected cells is generally viral DNA (10, 17), and the total acid-precipitable radioactivity in those supernatant fractions was, therefore, taken to represent synthesis of viral DNA in rate studies.

Inhibition of viral DNA synthesis by defective virus. BSC-1 cells were grown to confluency in 16-mm miniwells (ca. 8×10^4 cells per well). Wells were infected at different MOI with wild-type virus (776 or 777) in the presence and absence of CVP8/1/P4, a defective virus derived from 777. A 0.1-ml portion of undiluted defective virus stock was used. All infections were carried out in a total volume of 0.2 ml. After 2 h of adsorption at 37°C, the infection media were removed, Eagle no. 2 with 2% fetal bovine serum was added, and incubation at 37°C was continued. Thirty-six hours after infection, the cells were labeled for 1 h with 0.2 ml of fresh medium per well containing [^{3}H]-thymidine (20 μCi/ml). Viral DNA was isolated by the procedure of Hirt (10). Duplicate 50-μl aliquots of each Hirt supernatant (0.3 ml, total volume) were taken, treated as above, and counted.

Restriction endonuclease analyses. Strain 777 DNA was extracted from infected cells by the method of Hirt (10), and form I DNA was purified by two bandings in CsCl-ethidium bromide gradients (24). Strain 776 DNA was obtained directly from purified viral particles, and form I DNA was purified by one centrifugation in CsCl-ethidium bromide.

Endo R·*Hin*dII/R·*Hin*dIII were prepared by G.R.K.R. and Robert DiLauro; endo R·*Hae* III was prepared by R.D.; and endo R·*Alu* I was prepared by R.D. and A.C.K., using the methods of Smith and Roberts et al. (31, 26, 27, respectively). Endo R·*Eco*RI (Miles) was a commercial preparation.

Incubations contained, in a volume of 90 μl, 1 μg of DNA; in the case of mixed digests, 0.5 μg each of 776 and 777 form I DNA. Endo R·*Hin*dII/R·*Hin*dIII digests were carried out in the presence of a solution containing 6.6 mM Tris-hydrochloride (pH 7.5), 8.7 mM $MgCl_2$, and 35 mM NaCl. Endo R·*Hae* III digests contained a solution of 6 mM Tris-hydrochloride (pH 7.9), 6 mM $MgCl_2$, and 6 mM 2-mercaptoethanol, and endo R·*Alu* I digests contained 10 mM Tris-hydrochloride (pH 7.6)–7 mM $MgCl_2$–7 mM 2-mercaptoethanol. Incubations were started by adding sufficient enzyme to digest twice the amount of DNA present in an overnight incubation, as determined previously by titration. Incubation was carried out overnight at 37°C in stoppered tubes. Fresh enzyme was then added, and incubation was continued for several hours. The reaction was stopped by addition of 10 μl of a solution containing 2.5% sodium dodecyl sulfate (SDS), 60% glycerol, and 0.1% bromophenol blue.

Electrophoresis was carried out on polyacrylamide slab gels (16 by 14 by 0.15 cm). The 4%/6% gels were made by polymerising a 6% acrylamide solution (acrylamide-bisacrylamide, 25:1) in the bottom two-thirds of the gel and then a 4% solution (acrylamide-bisacrylamide, 20:1) in the top one-third of the gel. Other gels were made entirely with the 6% solution. Gels and running buffer contained 0.04 M Tris base–0.02 M sodium acetate–0.002 M EDTA brought to pH 7.8 with glacial acetic acid. Gels were prerun for at least 15 min at 100 V. Samples of digests containing between 0.2 and 0.5 μg of DNA were layered on the gel and were run at 100 V until the marker dye was at the bottom of the gel (3 to 5 h).

Gels were stained by immersing them in 500 ml of water containing 0.5 μg of ethidium bromide per ml for 25 min. Gels, supported by a quartz plate, were illuminated with a short-wave UV-light box (Mineralight, model C-51, Ultra-Violet Products Inc., San Gabriel, Calif.) and photographed through an A-23 filter (Kodak) with Polaroid 57 film. The intensity of the DNA bands is proportional to the concentration of nucleotide bases present, i.e., a large fragment will show a more intense band than a smaller fragment present in equimolar amounts. Therefore, a band having a greater intensity than that of a band migrating more slowly in the gel indicates the presence of more than one fragment in that band. Similarly, a low relative intensity indicates that a fragment is submolar with respect to other bands. Bands were identified as those characterized in previous work by both visual comparison of the relative size of bands on a single gel and by semilogarithmic plots of size against mobility.

Tryptic peptide analysis. Radioactive virus was prepared by infecting BSC-1 cells with either 776 or 777 (about 10 PFU/cell), adding labeled media from 20 to 92 h after infection, and then letting infection go to completion. Radioactive virus was purified from the lysates by the method of Pagano (24).

Strain 776 was labeled with both [^{14}C]lysine and [^{14}C]arginine (10 μCi of [^{14}C]lysine per ml, specific activity, 300 mCi/mmol and 5 μCi of [^{14}C]arginine per ml, specific activity, 312 mCi/mmol was used for labeling). Strain 777 was labeled in two parallel preparations, one with [^{3}H]lysine (using 10 μCi/ml; specific activity, 38.9 Ci/mmol) and the other batch with [^{3}H]arginine (10 μCi/ml; specific activity, 23 Ci/mmol).

The radioactive viral preparations were disrupted with SDS in 2-mercaptoethanol at 100°C and separated on SDS-polyacrylamide gels, using the system of Laemmli (14) with a 15% acrylamide running gel and a 4% stacking gel. The positions of the viral proteins were localized by autoradiography for the ^{14}C-labeled 776 and by fluorography (2) for the two ^{3}H-labeled preparations of 777. VP1 and VP2 run close together, but form distinct bands. To minimize contamination with VP2, only the top two-thirds of the VP1 bands was excised from the gels.

The gel slice containing the ^{14}C-labeled 776 VP1 was reswollen in 4 ml of 1% ammonium bicarbonate; the solution was discarded; 4 ml of fresh solution was added along with 160 μg of tolylsulfonyl phenylalanyl chloromethyl ketone (TPCK)-treated trypsin (Worthington), and the mixture was incubated overnight at 37°C. The ammonium bicarbonate solution was pipetted off and stored; 3 ml of fresh solution containing 90 μg of TPCK-treated trypsin was added; and incubation continued overnight. This solution was then

pipetted off and pooled with the first. The pool was centrifuged to remove small pieces of polyacrylamide and gel paper backing. A 25-μg amount of fresh trypsin was added to the supernatant fluid, and incubation was continued for 6 h. The solution was lyophilized to dryness, taken up in 10 ml of water, and lyophilized again. This procedure was repeated twice.

The gel slices containing the ^{3}H-labeled VP1s of the two 777 preparations were treated in the same way, except that the gel slices were first swollen in water and then soaked overnight in dimethyl sulfoxide to remove the 2,5-diphenyloxazole that was in the gels because of the fluorography procedure.

The tryptic peptides were analyzed on an Aminex A-5 (Bio-rad) column (0.2 by 15 cm, Altex), equilibrated in 0.05 N pyridine adjusted to pH 2 with formic acid at a temperature of 50°C (maintained by a circulating water jacket around the column), keeping a constant flow rate of 6 ml/h with a cheminert metering pump (Chromatronix), the pressure varying from 200 to 400 lb/in^2. Sample was applied in the same buffer with a sample loop attached directly to the top of the column, and the column was washed with this buffer. Fractions (0.25 ml) were collected directly into Biovial (Beckman) scintillation vials. After collecting 20 fractions, a linear gradient of starting buffer and 1 N pyridine, adjusted to pH 4.9 with acetic acid (15 ml of each), was passed through the column, followed by a wash with 1 N NaOH (about 7.5 ml). The column was regenerated by washing with a 10-ml solution of 0.2 N pyridine, 10 ml of 0.2 N pyridine-formate (pH 2) then 10 ml of starting buffer.

A 0.35-ml amount of water was added to each fraction followed by 3 ml of Aquasol (New England Nuclear), and samples were counted for 5 min each in a Beckman LS-355 liquid scintillation spectrometer. ^{3}H counts were corrected for ^{14}C spillover.

The methods for trypsinization directly in the gel slices and for the tryptic peptide analysis were kindly supplied by C. Cole of Stanford University.

RESULTS

DNA digestion with restriction endonucleases. Form I DNA (covalently closed superhelical circles) from SV40 strains 776 and 777 were digested either singly or together with either the combined endonucleases R · *Hin*dII/R · *Hin*dIII or with endonucleases R · *Hae* III or R · *Alu* I, and the digestion products were separated by electrophoresis on polyacrylamide gels (Fig. 1). This method will generally separate DNA fragments on the basis of size, but base composition may also influence mobility (19, 40). The various fragments observed and their estimated sizes are summarized in Table 1. The position of the various endonuclease fragments on the SV40 genome are shown in Fig. 2.

To piece together the results obtained with the various restriction endonucleases, we will start near the single endo R · *Eco*RI site on the SV40 genome (zero on the map in Fig. 2) and work clockwise, assuming that a difference of mobility in the gels indicates a difference in size. The endo R · *Hin*dIII/R · *Hin*dIII-F fragment of 777 is smaller than that of 776. The endo R · *Hae* III-B fragment (Fig. 2) is also smaller in 777 than in 776, and to about the same extent as the difference between the *Hin*dII/*Hin*dIII-F fragments (0.3 to 0.4% of the total SV40 genome length). The endo R · *Alu* I-L fragment of 776, which is fully contained within the endo R · *Hin*dII/R · *Hin*dIII-F region, is not seen in the 777 digests. The results are therefore consistent with a difference, probably a deletion of about 20 base pairs, between map positions 0.02 and 0.05. The endo R · *Eco*RI site at map position zero is present in both 777 and 776. However, the size of the endo R · *Alu* I-L fragment of 776 is 3.1% of the SV40 genome length (39), and, if the only difference in 777 was a 0.3 to 0.4% deletion, one would expect to see a fragment of about 2.6 to 2.7% in the endo R · *Alu* I digest of 777. It is possible that the extra material apparently associated with the endo R · *Alu* I-M, N region in 777 corresponds to the endo R · *Alu* I-L of 776, but several additional smaller fragments are also noted so that this region of 777 may be cleaved more extensively by endo R · *Alu* I than is 776. Also, the endo R · *Alu* I-E fragment is adjacent to the endo R · *Alu* I-L fragment, and the two submolar bands seen in the 777 digest, one moving equally with the 776 endo R · *Alu* I-E fragment, and one moving slightly slower, probably arise from this region (see below).

Next, the endo R · *Hae* III-C fragment of 777 is larger than that of 776. Endo R · *Alu* I-I, and -Q fragments seem to be identical in 776 and 777 (and both strains have the single endo R · *Bam* I site at position 0.17), but the endo R · *Alu* I-A fragment of 777 appears to be larger than that of 776. The difference would, therefore, lie between map positions 0.175 and 0.21. This region is contained within the endo R · *Hin*dII/R · *Hin*dIII-B fragment, and, in the mixed 776 and 777 digest, the endo R · *Hin*dII/R · *Hin*dIII-B fragments seem to separate slightly, providing further confirmation that this region is affected.

The endo R · *Alu* I-B fragment of 777 is larger than that of 776. This fragment is contained within the endo R · *Hin*dII/R · *Hin*dIII-A fragment and shares sequences with the endo R · *Hae* III-E and -A fragments. We do not see a difference between the endo R · *Hin*dII/R · *Hin*dIII-A fragments of 776 and 777, but a small difference in such a large fragment would not be readily noticeable. (In unpublished experiments, T. Vogel has observed that endo R · *Hin*dII/R · *Hin*dIII-A of 777 is slightly larger than the corresponding 776 frag-

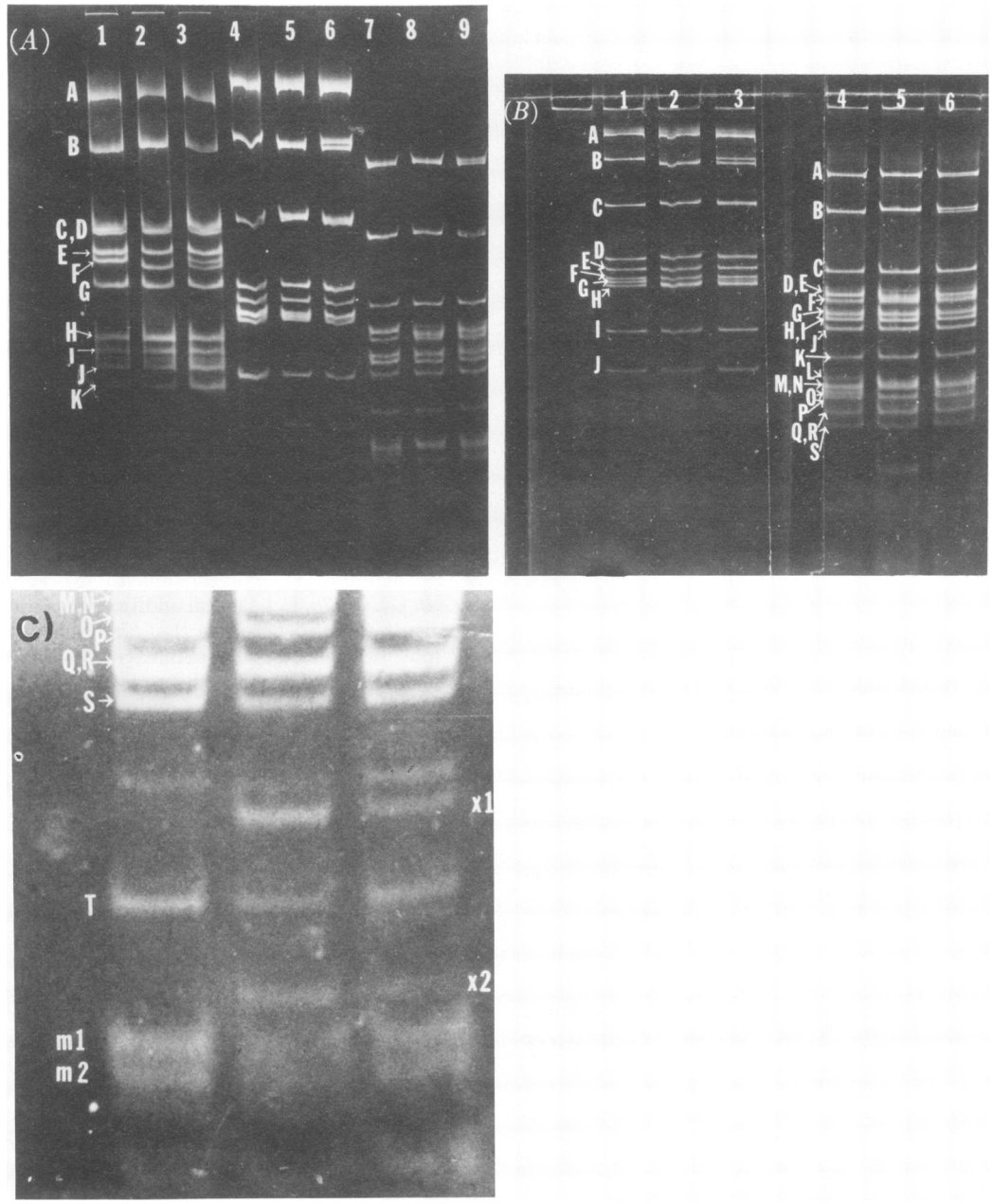

FIG. 1. *Polyacrylamide gel electrophoresis of restriction endonuclease fragments derived from 776 and 777 form I DNA with Endo R · HindII/R · HindIII, Endo R · Hae III, and Endo R · Alu I. (A) A 4%/6% polyacrylamide gel of restriction fragments produced by endo R · HindII/R · HindIII (slots 1 through 3), endo R · Hae III (slots 4 through 6), and endo R · Alu I (slots 7 through 9). In each series, the first slot contains a digest of 776 DNA, the second a digest of 777 DNA, and the third a mixed digest of both DNAs. Each sample contained about 0.3 μg of DNA. In slots 1 through 3 there appears to be some material migrating between the endo R · HindII/R · HindIII-I and -J fragments. This was not noted on other occasions and seems to be spurious. (B) A 6% polyacrylamide gel of restriction fragments produced by endo R · Hae III (slots 1 through 3) and endo R · Alu I (slots 4 through 6). The order of DNAs is the same as in Fig. 1A. Each sample contained about 0.3 μg of DNA. (C) The bottom portion of a 6% polyacrylamide gel of restriction fragments produced by endo R · Alu I. In this case, each sample contained about 0.45 μg of DNA, and the photograph was taken with a longer exposure.*

TABLE 1. *Comparison of restriction endonuclease fragments of SV40 strains 777 and 776*[a]

Endonuclease	Contents (%) 776	Fragment	777
*Hin*dII/III[b]	21.1	A	21.1
	15.4	B	15.9
	10.2	C	10.1
	10.1	D	10.1
	8.5	E	8.5
	8.4	F	8.0
	7.0	G	7.0
	5.2	H	5.2
	4.8	I	4.8
	4.5	J	4.5
	3.9	K	3.9
Hae III[c]	30.7	A	30.7
	15.7	B	15.1
	10.2	C	10.6
	7.0	D	7.0
	6.7	E	6.7
	6.3	F	6.3
	6.2	G	6.1
	6.1	H	6.1
	4.3	I	4.3
	3.3	J	3.3
Alu I[d]	14.0	A	14.2
	9.7	B	9.9
Alu I[d] (cont.)	6.5	C	6.5
	5.45	D	5.35
	5.45	E submolar	5.6
			5.45
	5.25	F	5.25
	4.7	G	4.7
	4.55	H	4.55
	4.50	I	4.50
	4.3	J	4.3
	3.6	K	3.6
	3.1	L	
	2.95	M	2.95
	2.87	N	2.87
	2.87	O	
	2.7	P	2.7
	2.5	Q	2.5
	2.5	R	2.5
	2.25	S	2.25
		X1 (probably a dimer)	1.7
	1.4	T	1.4
		X2 (possibly a dimer)	1.1
	1.0	M1 (dimer)	1.0
	0.9	M2 (dimer)	0.9

[a] Fragments in which differences are noted between 776 and 777 are underlined.

[b] Endo R · *Hin*dII/R · *Hin*dIII. The distances migrated by the various fragments in the gel (Fig. 1A) were measured. A semilog graph, using published values for the size of the endo R · *Hin*dII/R · *Hin*dIII fragments of 776 expressed as percentage of total SV40 genome length (38), was constructed, and the sizes of the 777 fragments were estimated. Certain of the size differences between fragments from 776 and 777 have been noted previously (19, 20).

[c] Endo R · *Hae* III. A similar graph was constructed using distances obtained in the 6% gel (Fig. 1B) and published values for the endo R · *Hae* III fragments of 776 (38). The sizes of the 777 fragments were estimated.

[d] Endo R · *Alu* I. A graph was constructed, using published values for the endo R · *Alu* I-A to -S fragments of 776 (39) but omitted the *Alu* I-B fragment. The published value for this fragment is 11.1% of the SV40 genome length. In our gel system, both the 776 and 777 *Alu* I-B fragments migrate considerably faster than expected for the 11.1% size. Therefore, our values for the *Alu* I-B fragments were calculated from the graph. For both 776 and 777, the sizes of fragments smaller than *Alu* I-S were estimated from Fig. 1C, using published values for the 776 *Alu* I-L to -S fragments. The endo R · *Alu* I-D to -F fragment region of the gel is complex. The endo R · *Alu* I-F fragments of 776 and 777 appear to be identical. The endo R · *Alu* I-D and -E fragments of 776 migrate together. In 777, a fragment runs behind the endo R · *Alu* I-F fragment but apparently faster than the 776 endo R · *Alu* I-D and -E fragments. There is another 777 endo R · *Alu* I fragment running equally with the 776 endo R · *Alu* I-D and -E fragments and also another fragment running just behind this position. These last two 777 fragments appear, from their intensity, to be submolar. These two submolar bands have been detected in endo R · *Alu* I digests of three different preparations of form I 777 DNA. All the DNAs were prepared from cells infected at low MOI with plaque-purified virus. Strain 777 appears to lack the endo R · *Alu* I-L and -O fragments found in 776 (Fig. 1B and C), and the 777 digest contains several small fragments, labeled X1 and X2, which appear, from their intensities, to contain more than one fragment and are not seen in the 776 digests. A previously unidentified band migrating between endo R · *Alu* I-S and X1 is seen in both 777 and 776 digests.

ment.) The same applies to the even larger endo R · *Hae* III-A fragments. With a smaller fragment, such as the endo R · *Hae* III-E fragment, we should be able to see this difference, but none is apparent on the gels. By elimination then, the difference lies between map positions 0.54 and 0.585. Another, less likely, explanation is that 777 is missing the endo R · *Alu* I site clockwise from the B fragment (39); however, the observed difference in size of the endo R · *Alu* I-B fragments of the two strains is not large enough to be explained in this way.

The endo R · *Hin*dII/R · *Hin*dIII-C fragment of 777 is smaller than that of 776. The situation

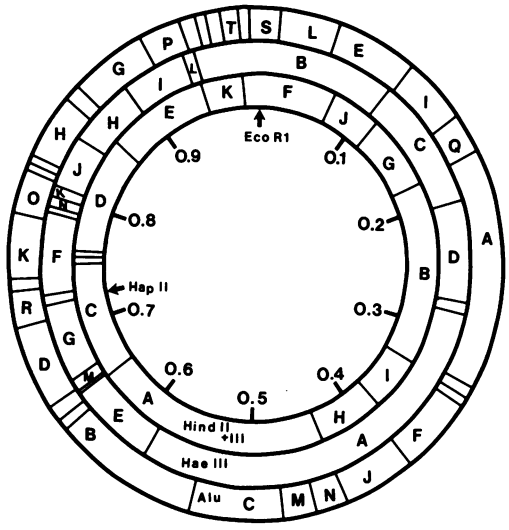

FIG. 2. *Circular map of the SV40 genome showing restriction endonuclease sites of 776 DNA. The map was drawn from data presented in references 5 and 37 for endo R · HindII/R · HindIII, reference 33 for endo R · Hae III, and in reference 39 for endo R · Alu I.*

is the same with the endo R · *Hae* III-G fragment of 777. The region of the SV40 genome in which the endo R · *Hae* III-G fragment is found has been shown to be anomalous upon endo R · *Hae* III digestion (12, 18), but the anomalies were attributed to the method of enzyme preparation rather than to the DNA used (18). In our case, since the same enzyme preparation was used on two DNAs, and since the mixed digest shows a mixed pattern, the differences appear to arise from the nature of the two DNAs. No difference can be seen in the endo R · *Alu* I-R fragments (and both 777 and 776 contain the single endo R · *Hap* II site located within *Alu* I-R), but, whereas in the 776 endo R · *Alu* I digest the -D and -E fragments ran together, in the 777 digest a fragment ran slightly faster. Considering the evidence of the endo R · *Hin*dII/R · *Hin*dIII and endo R · *Hae* III digests, this fragment probably arises from the endo R · *Alu* I-D region (which is why we consider that the two submolar bands observed in this region of the gel arise from the endo R · *Alu* I-E portion of the SV40 genome). The difference between the two strains, therefore, lies between the endo R · *Hae* III-M/-G junction and the endo R · *Alu* I-D/-R junction, i.e., between map positions 0.66 and 0.71.

Finally, the endo R · *Alu* I digest of 777 produces no fragment migrating at the position of the 776 endo R · *Alu* I-O fragment or any extra fragment migrating close by. There does not appear to be any significant difference between the two strains with respect to their endo R · *Hin*dII/R · *Hin*dIII-D fragments. Endo R · *Hae* III cuts this region of the SV40 genome into pieces too small for us to see on our gel. The simplest explanation is that in 777 the endo R · *Alu* I-O region contains at least one extra endo R · *Alu* I site, created possibly by a single base pair change, and that some of the small endo R · *Alu* I fragments found in 777 but not in 776 arise from this region of the genome.

Peptide analysis. The endo R · *Alu* I-L and -E fragments lie in that part of the SV40 genome that codes for the major viral capsid protein VP1 (27, 35). We, therefore, analyzed the tryptic peptides obtained from purified VP1s of both 776 and 777. One (776) was labeled simultaneously with both [^{14}C]lysine and [^{14}C]arginine in order to label all the tryptic peptides. The other virus (777) was labeled in two parallel preparations with either [^{3}H]lysine or [^{3}H]arginine. VP1 contains about 40 to 50 lysines and arginines (34).

The pattern observed with VP1s from 776 and 777, labeled in both lysine and arginine (the two ^{3}H-labeled 777 preparations were mixed in this experiment), are shown in Fig. 3. It can be seen that while the patterns are basically similar, there are several differences. The 776 preparation has a peptide eluting just before peak 1 of 777. This is reflected in a low ^{3}H-^{14}C ratio in this region. The 776 VP1 appears to lack both peaks 5 and 7 found in the VP1 of 777. Also, from the ^{3}H-^{14}C ratio, 777 appears to have an extra peptide in peak 10. From similar columns run with VP1 from 777 labeled only in either lysine or arginine, all the peptides found in 777 but not in 776 VP1 are lysine peptides (data not shown). Since there are so many peptides, counts never really fell to base line levels, making it impossible to quantify accurately the number of peptides in a peak. It seems, however, that the 777 VP1 is missing one peptide found in the 776 VP1 but has at least three additional lysine peptides. Such a pattern cannot arise if the only difference between the DNAs of 776 and 777 in the region coding for their respective VP1s is a simple deletion in the *Alu*-L fragment of 777.

Physiological comparison of strains 776 and 777. Figure 4 shows the rate of viral DNA synthesis at various times after infection of the BSC-1 line of monkey kidney cells with either strain 776 or 777 at an MOI of 10 PFU/cell. The rates were estimated by means of 1-h labeling periods with [^{3}H]thymidine. Other experiments (data not shown) indicated that the incorporation of [^{3}H]thymidine into viral DNA of either strain is linear from time zero of the pulse

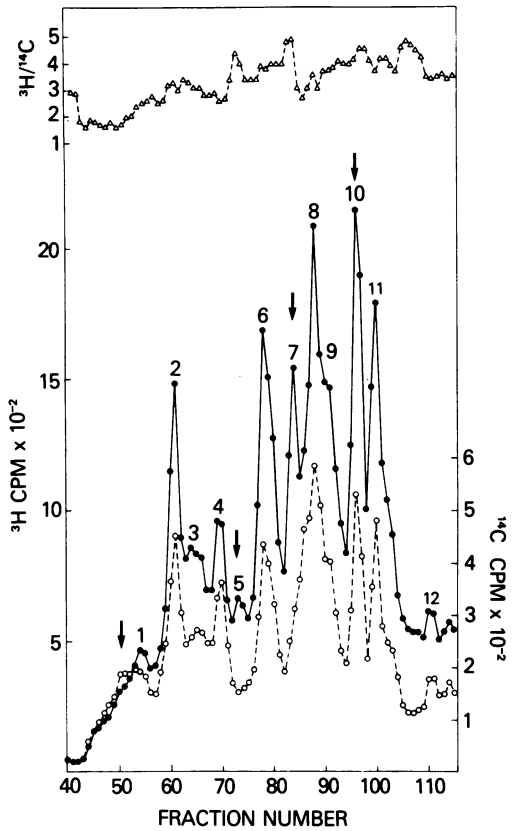

FIG. 3. *Tryptic peptide patterns of VP1s from strains 776 and 777. One preparation of VP1 of 776 labeled in both lysine and arginine with ^{14}C and two preparations of VP1 from 777, one labeled with [^3H]lysine and the other with [^3H]arginine, were purified and digested with trypsin. The figure shows the peptide patterns obtained on an Aminex-A5 column for a mixture of the ^{14}C-labeled VP1 of 776 and the [^3H]lysine- and [^3H]arginine-labeled VP1s of 777. The input ratio of [^3H]lysine-to-[^3H]arginine counts in the mixture was 4.7:1; this ratio was calculated considering the ratio of [^{14}C]lysine to [^{14}C]arginine used in the preparation of VP1 of 776 and the published ratio of lysine to arginine residues in the VP1 of 777 (9). ●, ^3H counts; ○, ^{14}C counts; △, ^3H-^{14}C ratio for each fraction. The peaks observed with 777 VP1 are numbered, and arrows indicate differences observed between the two patterns.*

up to at least 1 h and, further, that the rate is dependent on MOI up to a value of 50 PFU/cell (25). The observed rates of DNA synthesis are similar with both 776 and 777 at all times after infection. However, there is a marked difference in yield of the two viruses obtained from complete infection of a cell monolayer. If infection is made at a very low MOI (about 10^{-3} PFU/cell) and is allowed to continue until full cytopathic effects are observed, then 776 consistently yields only about one-tenth to one-fourth the number of PFUs that one obtains with 777 (in this laboratory typically about 10^8 PFU/ml of lysate for 776 and 10^9 PFU/ml for 777, or about 250 and 2,500 PFU produced per cell). These numbers are higher than, but consistent with, differences that Takemoto et al. observed with small- and large-plaque SV40 variants on infection of primary African green monkey kidney cells (34).

Defective interfering viruses have been found to arise with many animal viruses, and, in several instances, interference by defective viruses has been shown to be specific for a homologous virus system (11). We have observed such a specificity by comparing the effect of defective virus derived from strain 777 on the replication of wild-type strains 777 and 776 viral DNA. Coinfection of BSC-1 cells with wild-type plaque-purified 777 SV40 and a defective variant derived from serial undiluted passage of strain 777 (designated CVP8/1/P4 [25]), results in almost complete inhibition, at all MOI tested, of the rate of viral DNA synthesis compared with that observed with wild-type infection alone (Table 2). However, as shown in Table 2, the same concentrations of 777-derived defective inhibit 776 DNA synthesis to a much lesser extent. In other ex-

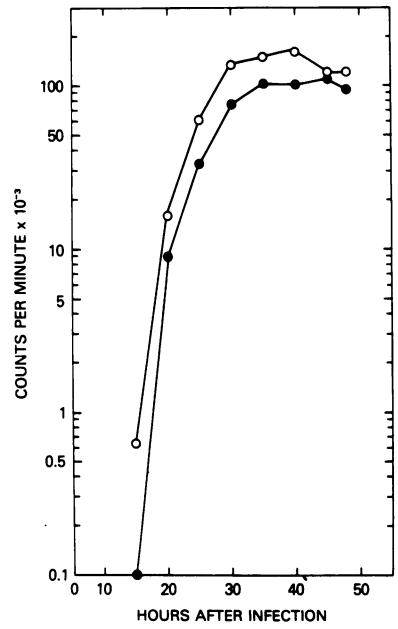

FIG. 4. *Comparison of rates of viral DNA synthesis after infection with strains 776 and 777. Confluent monolayers of BSC-1 cells were infected with strain 776 or strain 777 at an MOI of 10. The cells were labeled with [^3H]thymidine at indicated times after infection. The values are corrected for incorporation in mock-infected cells.* ○, *776;* ●, *777.*

TABLE 2. *Inhibition of viral DNA synthesis by defective virus*[a]

Wild-type virus	MOI	CVP8/1/P4	Expt 1		Expt 2	
			cpm/50 μl	% Inhibition	cpm/50 μl	% Inhibition
777	1	−	212		226	
	5	−	1,576		1,509	
	10	−	2,988		2,757	
	20	−	6,391		4,588	
777	1	+	0	100	0	100
	5	+	0	100	0	100
	10	+	32	99	0	100
	20	+	247	96	86	98
776	1	−	514		355	
	5	−	2,777		2,035	
	10	−	3,895		3,883	
	20	−	5,551		5,648	
776	1	+	255	50	83	77
	5	+	1,092	61	387	81
	10	+	2,423	38	2,299	41
	20	+	2,857	49	4,096	27

[a] BSC-1 cells were infected with either 776 or 777 at the MOI shown in the presence or absence of CVP8/1/P4, a 777-derived defective virus (0.1 ml of undiluted defective virus stock per 8×10^4 cells). Thirty-six hours after infection, cells were pulsed for 1 h with [^{3}H]thymidine, viral DNA was extracted by the method of Hirt (10), and two 50-μl aliquots of each Hirt supernatant fraction (out of a total volume of 0.3 ml) were counted. The values in the table are the averages for the two aliquots. Inhibition of viral DNA synthesis is calculated for each MOI of wild-type virus. The counts per minute of 50 μl incorporated into similar samples from mock-infected control cells have been subtracted (358 cpm/50 μl in experiment 1; 315 cpm/50 μl in experiment 2). Infection with CVP8/1/P4 alone gave 203 cpm/50 μl in experiment 1 and 121 cpm/50 μl in experiment 2.

periments (not shown), at concentrations of CVP8/1/P4 or CBV/1/P8 (another 777-derived defective) that inhibited 777 DNA synthesis by 70%, there was no inhibition at all of 776 DNA synthesis.

DISCUSSION

Differences between the DNAs of the SV40 variants 776 and 777 have been detected at five distinct points of the SV40 genome by restriction endonuclease analysis. The most obvious difference, and one that has been reported in passing several times (19, 20), is a deletion of about 0.5% of the SV40 genome in the endo R · *Hin*dII/R · *Hin*dIII-F fragment of 777. We can now localize the defect more precisely within the endo R · *Alu* I-L fragment between map positions 0.02 and 0.05. This is within the region known to code for the major capsid protein VP1, and, indeed, the tryptic peptide patterns of VP1s from 776 and 777 are different to some extent. However, the differences observed, with 777 lacking one of the 776 VP1 tryptic peptides but having at least three additional ones, cannot be accounted for by a simple deletion. With a simple deletion that did not involve any lysine or arginine residues, the two proteins would have the same number of tryptic peptides, but with one being altered. If the deletion involved arginines or lysines, then the 777 VP1 would have fewer tryptic peptides than the VP1 of 776. That something more than a simple deletion is involved is also indicated by the appearance of two submolar bands in the endo R · *Alu* I digest of 777 DNA. These submolar bands probably arise from the region corresponding to the endo R · *Alu* I-E fragment of 776, a region that is adjacent to the endo R · *Alu* I-L fragment and is also involved in coding for VP1. The reason for the submolar amounts is not known, but it might reflect variation in the modification of bases in this region. Complex differences between the capsid protein genes of 776 and 777 are also suggested by complementation tests. Strain 777 is a temperature-sensitive variant that grows poorly at 40–41°C (21; Y. Gluzman, E. Kuff, and E. Winocour, submitted for publication). Whereas 777 can fully complement *tsA*30 mutants at 40 to 41°C, it does not complement *tsB*204 or *tsC*219 mutants (Gluzman, Kuff, and Winocour, submitted for publication). *tsB*204 maps in the endo R · *Hin*dII/R · *Hin*dIII-F fragment, and *tsC*219 maps in the endo R · *Hin*dII/R · *Hin*dIII-J fragment (15), which contains most of the endo R · *Alu* I-E fragment (Fig. 2). While it is possible that 777 is a mutant of the *tsBC* type, most of which map in the endo R · *Hin*dII/R · *Hin*dIII-G fragment (14), our data suggest that it is a double mutant with defects in both the endo R · *Alu* I-L and -E regions.

Other differences between 777 and 776 are located at map positions 0.175 to 0.21 and 0.54 to 0.585. The former difference is at or near the termination point for replication (4) and for early (13) and late (6) transcription, whereas the latter difference is contained within the early region of transcription (15). Interestingly, both differences are located in regions that are not necessary for viable growth (19, 30). The viable deletion mutants were not tested for temperature sensitivity.

Another difference is found in the region 0.66 to 0.71, near the origin of DNA replication (4, 8). Viable deletions have also been mapped in this region (19, 30), and large tandem repeats of nucleotide sequences occur in this region (6).

Finally, there is a difference between the two strains in their endo R · *Alu* I-O fragments. This

difference may well be minor, perhaps involving only a single base pair change resulting in an extra endo R · *Alu* I site in this region of 777 DNA. There may be little or no repercussion upon the viral protein VP2 coded for by this region (29).

Restriction endonuclease analysis only reveals differences in nucleotide sequences related to the specific cleavage sites. Clearly, other sequence alterations may be involved in the phenotypic differences between viral strains. Only comparative sequence analysis can resolve these details.

Strain 776 is a small-plaque variant of SV40. In our hands, 777 generally gives larger plaques than 776, although the 777 plaques vary in size. In addition, temperature sensitivity, deletion in the endo R · *Hin*dII/R · *Hin*dIII-F fragment, and altered coat protein all suggest that 777 is related to the large-plaque strains previously studied (1, 20, 34). Large-plaque strains are reported to be more oncogenic than small-plaque strains (34), are immunologically distinct (23), and are more restricted in host range (22). Many of these differences are probably related to the differences in the gene that codes for the major coat protein. Host restriction may involve an early step in infection, a block in penetration, or uncoating of the virus particle (22). Strain 777, having a different capsid than 776, may not be so well recognized by receptors on the cell surface. That different strains are immunologically distinct suggests that differences in the capsids are expressed on the surface of the virus. This would be understandable, since the capsid is a complex structure and it would be more difficult to alter markedly those parts of the protein involved in interactions with its neighbors and still maintain the specific viral structure. That the endo R · *Alu* I-L and -E fragment region of the DNA codes for an exterior part of the virus is also indicated by the altered surface charge of the *tsB*204 mutant (41).

Other differences between 776 and 777 are their plaque morphology and the lower apparent yield of 776, even though the rates of 777 and 776 viral DNA synthesis observed at a given MOI are very similar. Both phenomena may be related to the altered capsid. If, because of its capsid, 776 adheres to cells more efficiently than 777, then, although the actual burst size of the two viruses may be similar, more newly synthesized 776 may be used up in subsequent reinfections than is the case with 777. After all the cells in the monolayer have been killed, the apparent yield of 776 would be lower. Another factor could be a greater loss of 776 by adsorption to cell debris. Similarly, if 777 adsorbs less efficiently than 776, then released 777 virions may have a greater opportunity to diffuse, thereby spreading the area of subsequent infections and leading to a larger plaque size. A similar explanation has previously been offered for small- and large-plaque variants of polyoma (7).

The specificity of the phenomenon of interference by defective virions is also observed with 776 and 777. Again, this may be related to differences in the capsids, with defectives bearing the 777 capsid being unable to compete effectively with wild-type 776 for adsorption. However, in other defective interfering virus systems, adsorption does not seem to be the site of the effect (11). It is interesting that one of the differences observed between 776 and 777 occurs near the origin of DNA replication. It is, perhaps, this difference that prevents defectives derived from 777 from interfering with the replication of 776.

Finally, we would stress the importance of recognizing that the various SV40 strains in use in different laboratories may contain multiple differences in their genomes. Given the widespread and necessary practice of plaque purification, even those strains considered of common origin may have developed differences over the years.

ACKNOWLEDGMENTS

We are grateful to Ernest Winocour and Tikva Vogel and their colleagues, for making their data available to us before publication, and to C. Cole, for advice concerning the tryptic peptide analysis.

LITERATURE CITED

1. **Barban, S.** 1973. Electrophoretic differences in the capsid proteins of simian virus 40 plaque mutants. J. Virol. **11**:971-977.
2. **Bonner, W. M., and R. A. Laskey.** 1974. A film detection method for tritium-labelled proteins and nucleic acids in polyacrylamide gels. Eur. J. Biochem. **46**:83-88.
3. **Chou, J. Y., and R. G. Martin.** 1974. Complementation analysis of simian virus 40 mutants. J. Virol. **13**:1101-1109.
4. **Danna, K. J., and D. Nathans.** 1972. Bidirectional replication of simian virus 40 DNA. Proc. Natl. Acad. Sci. U.S.A. **69**:3097-3100.
5. **Danna, K. J., G. H. Sack, Jr., and D. Nathans.** 1973. Studies of simian virus 40 DNA. VII. A cleavage map of the SV40 genome. J. Mol. Biol. **78**:363-376.
6. **Dhar, R., K. N. Subramanian, J. Pan, and S. M. Weissman.** 1977. Structure of a large segment of the genome of simian virus 40 that does not encode known proteins. Proc. Natl. Acad. Sci. U.S.A. **74**:827-831.
7. **Diamond, L., and L. V. Crawford.** 1964. Some characteristics of large-plaque and small-plaque lines of polyoma virus. Virology **22**:235-244.
8. **Fareed, G. C., C. F. Garon, and N. P. Salzman.** 1972. Origin and direction of simian virus 40 deoxyribonucleic acid replication. J. Virol. **10**:484-491.
9. **Greenaway, P. J., and D. LeVine.** 1973. Amino acid compositions of simian virus 40 structural proteins.

Biochem. Biophys. Res. Commun. **52**:1221-1227.
10. **Hirt, B.** 1967. Selective extraction of polyoma DNA from infected mouse cell cultures. J. Mol. Biol. **26**:365-369.
11. **Huang, A. S.** 1973. Defective interfering viruses. Ann. Rev. Microbiol. **27**:101-117.
12. **Jay, E., and R. Wu.** 1976. *Arthrobacter luteus* restriction endonuclease recognition sequence and its cleavage map of SV40 DNA. Biochemistry **15**:3612-3620.
13. **Khoury, G., P. Howley, D. Nathans, and M. Martin.** 1975. Posttranscriptional selection of simian virus 40-specific RNA. J. Virol. **15**:433-437.
14. **Laemmli, U. K.** 1970. Cleavage of structural proteins during the assembly of the head of bacteriophage T4. Nature (London) **227**:680-685.
15. **Lai, C. J., and D. Nathans.** 1975. A map of temperature-sensitive mutants of simian virus 40. Virology **66**:70-81.
16. **Lavi, S., and E. Winocour.** 1972. Acquisition of sequences homologous to host DNA by closed circular simian virus 40 DNA. J. Virol. **9**:309-316.
17. **LeBlanc, D. J., and M. F. Singer.** 1974. Localization of replicating DNA of simian virus 40 in monkey kidney cells. Proc. Natl. Acad. Sci. U.S.A. **71**:2236-2240.
18. **Lebowitz, P., W. Siegel, and J. Sklar.** 1974. *Hemophilus aegyptius* restriction endonuclease cleavage map of the simian virus 40 genome and its colinear relation with the *Hemophilus influenzae* cleavage map of SV40. J. Mol. Biol. **88**:105-123.
19. **Mertz, J. E., and P. Berg.** 1974. Viable deletion mutants of simian virus 40: selective isolation by means of a restriction endonuclease from *Hemophilus parainfluenzae*. Proc. Natl. Acad. Sci. U.S.A. **71**:4879-4883.
20. **Nathans, D., and K. J. Danna.** 1972. Studies of SV40 DNA. III. Differences in DNA from various strains of SV40. J. Mol. Biol. **64**:515-518.
21. **Ossowski, L.** 1972. The effect of high temperature on biological functions of three strains of SV-40. Virology **49**:612-614.
22. **Ozer, H. L., and K. K. Takemoto.** 1969. Site of host restriction of simian virus 40 mutants in an established African green monkey kidney cell line. J. Virol. **4**:408-415.
23. **Ozer, H. L., K. K. Takemoto, R. L. Kirschstein, and D. Axelrod.** 1969. Immunochemical characterization of plaque mutants of simian virus 40. J. Virol. **3**:17-24.
24. **Pagano, S. P., and C. A. Hutchison III.** 1971. Small circular viral DNA: preparation and analysis, p. 79-123. *In* K. Maramorosch and H. Koprowski (ed.), Methods in virology, vol. 5. Academic Press Inc., New York.
25. **Rao, G. R. K., and M. F. Singer.** 1977. Studies on a defective variant of simian virus 40 that is substituted with DNA sequences derived from monkey. I. Origin, properties, and purification. J. Biol. Chem. **252**:5115-5123.
26. **Roberts, R. J., J. B. Breitmeyer, N. F. Tabachnik, and P. A. Myers.** 1975. A second specific endonuclease from *Haemophilus aegyptius*. J. Mol. Biol. **91**:121-123.
27. **Roberts, R. J., P. A. Myers, A. Morrison, and K. Murray.** 1976. A specific endonuclease from *Arthrobacter luteus*. J. Mol. Biol. **102**:157-165.
28. **Rozenblatt, S., S. Lavi, M. F. Singer, and E. Winocour.** 1973. Acquisition of sequences homologous to host DNA by closed circular simian virus 40 DNA. III. Host sequences. J. Virol. **112**:501-510.
29. **Rozenblatt, S., R. C. Mulligan, M. Gorecki, B. E. Roberts, and A. Rich.** 1976. Direct biochemical mapping of eukaryotic viral DNA by means of a linked transcription-translation cell-free system. Proc. Natl. Acad. Sci. U.S.A. **73**:2747-2751.
30. **Shenk, T. E., J. Carbon, and P. Berg.** 1976. Construction and analysis of viable deletion mutants of simian virus 40. J. Virol. **18**:664-671.
31. **Smith, H. O.** 1974. Restriction endonuclease from *Hemophilus influenzae* RD. Methods Mol. Biol. **7**:71-85.
32. **Smith, H. O., and D. Nathans.** 1973. A suggested nomenclature for bacterial host modification and restriction systems and their enzymes. J. Mol. Biol. **81**:419-423.
33. **Subramanian, K. N., J. Pan, S. Zain, and S. M. Weissman.** 1974. The mapping and ordering of fragments of SV40 DNA produced by restriction endonucleases. Nuc. Acids Res. **1**:727-752.
34. **Takemoto, K. K., R. L. Kirschstein, and K. Habel.** 1966. Mutants of simian virus 40 differing in plaque size, oncogenicity, and heat sensitivity. J. Bacteriol. **92**:990-994.
35. **Tegtmeyer, P., and H. L. Ozer.** 1971. Temperature-sensitive mutants of simian virus 40 infection of permissive cells. J. Virol. **8**:516-524.
36. **Van de Voorde, A., R. Contreras, R. Rogiers, and W. Fiers.** 1976. The initiation region of the SV40 VP1 gene. Cell **9**:117-120.
37. **Yang, R., K. Danna, A. Van De Voorde, and W. Fiers.** 1975. Location of the small restriction fragments, Hind-L, Hind-M and Hpa-E, on the simian virus 40 genome. Virology **68**:260-265.
38. **Yang, R. C. A., A. Van de Voorde, and W. Fiers.** 1976. Cleavage map of the simian-virus-40 genome by the restriction endonuclease III of *Haemophilus aegyptius*. Eur. J. Biochem. **61**:101-117.
39. **Yang, R. C. A., A. Van de Voorde, and W. Fiers.** 1976. Specific cleavage and physical mapping of simian-virus-40 DNA by the restriction endonuclease of *Arthrobacter luteus*. Eur. J. Biochem. **61**:119-138.
40. **Zeiger, R. S., R. Salomon, C. W. Dingman, and A. C. Peacock.** 1972. Role of base composition in the electrophoresis of microbial and crab DNA in polyacrylamide gels. Nature (London) New Biol. **238**:65-69.
41. **Zweig, M., S. Barban, and N. P. Salzman.** 1976. Analysis of simian virus 40 wild-type and mutant virions by agarose gel electrophoresis. J. Virol. **17**:916-923.